PHYSICAL REVIEW B VOLUME 51, NUMBER 19 15 MAY 1995-I

Single electron switching in a parallel quantum dot

F. Hofmann, T. Heinzel,* D.A. Wharam, and J.P. Kotthaus
Ludwig-Maximilians Universität, Geschwister-Scholl-Platz 1, D 80539, München, Germany

G. Böhm, W. Klein, G. Tränkle, and G. Weimann
Walter Schottky Institut, Technische Universität München, D 85748 Garching, Germany
(Received 30 December 1994)

Low-temperature conductance measurements have been performed upon a parallel quantum-dot configuration defined in the two-dimensional electron gas of a GaAs-$Al_xGa_{1-x}As$ heterostructure. The observed Coulomb-blockade oscillations of the conducting dot exhibit pronounced periodic shifts as a consequence of the tunable coupling to the nonconducting dot. We show that the transport is essentially determined by the interdot capacitance and that the addition of a single electron to the nonconducting dot can switch the device conductance from a maximum to a Coulomb-blockade minimum.

Investigations of the Coulomb blockade (CB) of transport in small mesoscopic structures have aroused much recent interest not only because of the fascination of the fundamental physical effects but also because of the significant technological implications for future mesoscopic devices. The possibility to exactly tune the number of electrons in the active region of a device has led to the development of both the single electron turnstile[1] as well as the electron pump.[2] A common feature of all such devices is their extreme sensitivity to the immediate electrostatic environment which results essentially from the scale of the typical capacitances. The transport properties are consequently dominated by the large Coulomb charging energies. In a single quantum dot this leads to the observation of conductance oscillations as the electrochemical potential of the dot is tuned.[3] More recently it has been suggested that it may be possible to realize a cellular automata device in a configuration of coupled quantum dots.[4] In this device the switching results from the change in the quantum-mechanical ground-state configuration arising from externally imposed polarization charges. In order to realize such a device an understanding of both the Coulomb interaction and the quantum-mechanical tunneling between coupled quantum dots is essential. Recent investigations of serial double-dot configurations manifest the so-called stochastic CB;[5–7] however here the requirement that the CB be simultaneously lifted in both dots complicates the detailed analysis of the observed conductance oscillations.

Here we report upon low-temperature experimental investigations performed upon a double quantum-dot structure arranged in a parallel configuration. This has the advantage that the electronic transport is through a single quantum dot and the resulting CB oscillations (CBO's) permit a direct determination of a change in the number of electrons in this quantum dot. We demonstrate that the device conductance can be switched from a CB maximum to a minimum by the addition of a single electron to the adjacent nonconducting dot. The structure [see Fig. 1(a)] is defined by the application of negative gate biases to electrodes defined lithographically on the surface of a GaAs-$Al_xGa_{1-x}As$ heterostructure. The two-dimensional (2D) electron gas is situated 60 nm below the sample surface and has a low-temperature mobility and density of 1.1×10^6 cm^2/V s and 3.6×10^{15} m^{-2}, respectively. The main dot, through which the current flows, is weakly coupled to the surrounding source and drain reservoirs via quantum point contacts (QPC's). Each QPC is tuned via a pair of electrodes (Q_i,F_i) with the voltages chosen such that the conductance through the QPC is less than e^2/h. In addition the main dot is coupled to the second dot via an additional QPC which can be continuously tuned via the voltages applied to F_1 and F_2. Both dots are further controlled via a central electrode (C_i) which simultaneously tunes both the electrochemical potential and dot geometry.

The completed device was inserted directly into the mixing chamber of our top-loading dilution refrigerator. All measurements were performed at the base temperature of the cryostat ($T_{\text{bath}}=25$ mK) and a small ac excitation voltage, typically 10 μV, was applied between the source and drain reservoirs and the conductance of the device measured using low-frequency ($f_0=33$ Hz) phase-sensitive detection.

Initial experiments were performed to characterize the internal QPC between the main and second dot. With the second center gate grounded ($V_{C_2}=0$ V) the CBO's of the main dot, observed when V_{C_1} is swept, were used to determine the dot configuration. For electrode voltages $V_{F_1}=V_{F_2}>-475$ mV no CBO's are observed; the main dot is well coupled to a large 2D reservoir and hence the charging energy of the internal region is insignificant compared with k_BT. As V_{F_1} and V_{F_2} are further decreased clear CBO's are observed demonstrating the definition of a tunnel barrier between the dot and the adjacent 2D region. Initially these CBO's are quite broad due to the dot-reservoir coupling; however the oscillations sharpen as V_{F_1},V_{F_2} are decreased until, at a voltage of approximately -520 mV, no further variation is observed. The tunnel barrier between the main dot and the adjacent 2D reservoir is now so large that there is effectively no coupling and the conductance of the device reflects that of a single quantum dot.

Having defined a range of voltages for which the coupling between the two dots is significant, systematic measurements of the dot conductance were then performed with fixed val-

0163-1829/95/51(19)/13872(4)/$06.00 © 1995 The American Physical Society

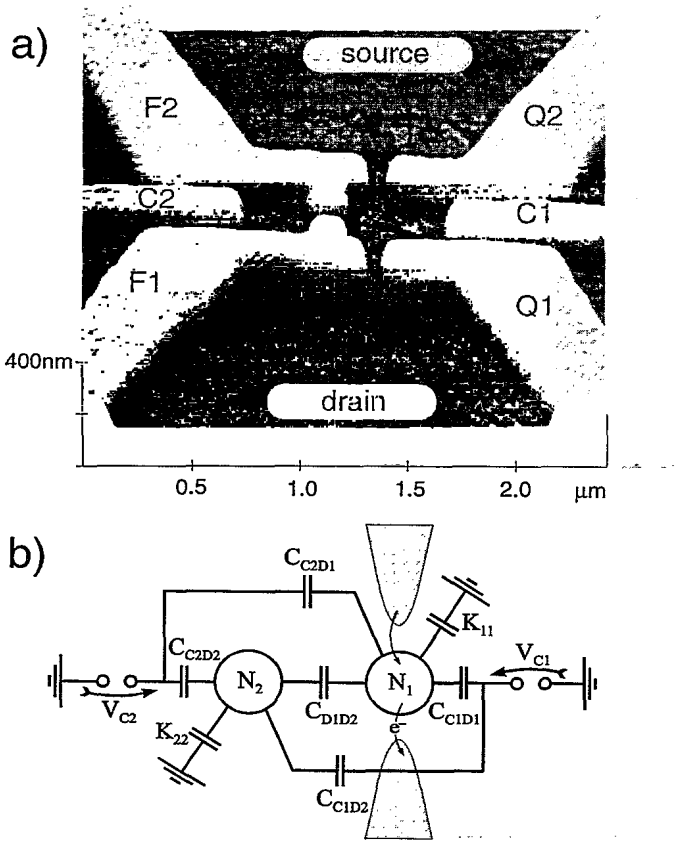

FIG. 1. (a) An atomic force image of the device structure used in the experiments. The outer electrodes define both the quantum point contacts coupling the main dot to the reservoirs as well as the inner quantum point contact which controls the interdot coupling. The geometries of the two dots can be independently tuned with the two center gates. The labels used refer to the notation of the text. (b) The equivalent circuit used to model the parallel dot structure; the total charge on each dot is separately quantized as expected in the CB regime, the center gates determine the magnitude of the $C_{C_iD_j}$ partial capacitances, while the interdot capacitance $C_{D_1D_2}$ depends upon the finger-gate voltage $V_{F_{1,2}}$. The remaining partial capacitances are included in the capacitances K_{11} and K_{22}.

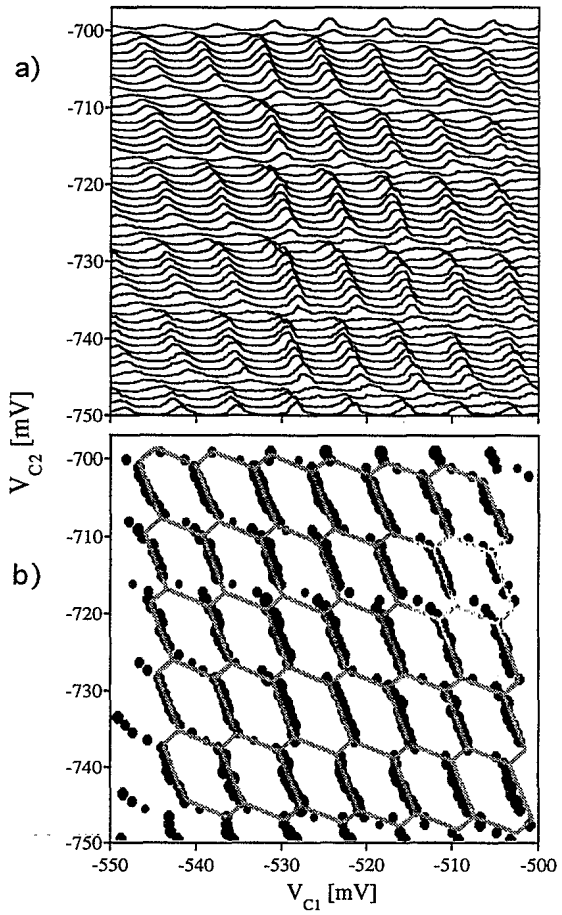

FIG. 2. (a) Typical conductance measurements for the parallel dot structure shown in Fig. 1. Each trace corresponds to a fixed value of second center-gate voltage, V_{C_2}; the curves are offset vertically with an offset given by the magnitude of V_{C_2}. The conductance scale is arbitrary but constant over the whole range of measurements. The bath temperature was 25 mK and the applied finger-gate voltage $V_{F_1}=V_{F_2}=-485$ mV. (b) The conductance maxima of (a) are plotted as a function of the two center-gate voltages and, in addition, the calculated phase diagram resulting from the capacitance model discussed in the text.

ues of V_{C_2}. Typical experimental results are shown in Fig. 2(a); each curve denotes a different value of V_{C_2} and it is clear that changing the second center-gate voltage results not only in a shift of the conductance peak positions but also in a periodic modification of the absolute value of conductance. This reduction of the conductance appears at values of V_{C_2} where the peak positions seem to jump.

In order to understand this structure in detail we have modeled the device using a classical capacitance model. The equivalent circuit assumed is illustrated in Fig. 1(b); in accordance with other authors,[2,9] we have minimized the total energy stored in the system of capacitances with the additional constraint that the number of electrons confined to the two quantum dots is independently quantized. Under the assumption that the partial capacitances are independent of the applied center-gate voltages the resulting expression for the total energy is given by

$$W_{DQD}(N_1,N_2,V_{C_1},V_{C_2}) = \tfrac{1}{2}\Delta Q^T \begin{pmatrix} C_{\Sigma D_1} & -C_{D_1D_2} \\ -C_{D_1D_2} & C_{\Sigma D_2} \end{pmatrix}^{-1} \Delta Q \quad (1)$$

with

$$\Delta Q = \begin{pmatrix} eN_1 - C_{C_1D_1}V_{C_1} - C_{C_2D_1}V_{C_2} \\ eN_2 - C_{C_2D_2}V_{C_2} - C_{C_1D_2}V_{C_1} \end{pmatrix}.$$

Here the capacitances are defined as in Fig. 1(b) and $C_{\Sigma D_i}$ are the total dot capacitances. This formula may be intuitively understood as the total energy stored on the dot structure as a result of the difference between the quantized charge in the dots and the continuous charge induced by the external voltage sources. From the above expression it is clear that the energetically stable electronic configuration

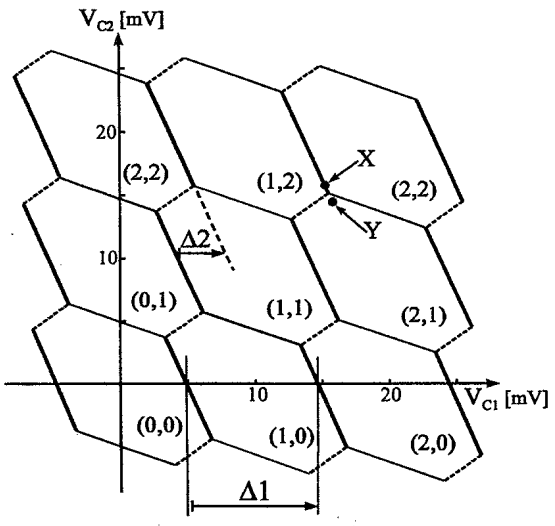

FIG. 3. The periodic structure of the phase diagram is clearly illustrated and the configuration (N_1,N_2) of the structure indicated. The three fundamentally different types of phase boundary are indicated; the relationship between the phase-boundary separations (Δ_i) and the partial capacitances is discussed in the text. The partial capacitances have been chosen such that the periodic structure agrees with a typical measurement.

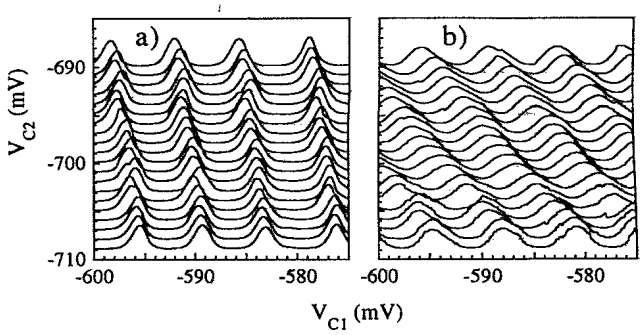

FIG. 4. Conductance measurements for two limiting cases of interdot coupling are shown. (a) For $V_{F_1}=V_{F_2}=-520$ mV the coupling between the dots is essentially removed and the capacitance $C_{D_1D_2}$ is negligible. The slight shift of the peak positions with decreasing V_{C_2} is caused by the small cross capacitance $C_{C_2D_1}$ and is approximately 2 aF. (b) Conductance measurements for the same range of center-gate voltages are shown for $V_{F_1}=V_{F_2}=-470$ mV. The two dots have merged into a large single dot whose total electron number can be tuned by each electrode separately.

(N_1,N_2) of the parallel quantum dot depends critically upon the two center-gate voltages and upon the magnitude of the partial capacitances. The points of degeneracy $[W_{DQD}(N_1,N_2,V_{C_1},V_{C_2})=W_{DQD}(N_1\pm1,N_2\pm1,V_{C_1},V_{C_2})]$ between adjacent configurations permit the construction of a "phase diagram" as has been studied previously in the context of the electron pump[2] and a single quantum dot in a high magnetic field.[8,9] For the parallel quantum-dot structure discussed here the significance of the phase diagram is twofold: first, the phase boundaries which are visible in a conductance sweep are those where the total number of electrons (N_1+N_2) in the parallel dot structure change by one; and second, the precise shape of the periodic cell in the phase diagram is tunable through the interdot capacitance. The character of this phase diagram is illustrated in Fig. 3 where several periods are plotted as a function of the voltages applied to the two center gates. The voltage separations shown between the various phase boundaries are analytic functions of the system capacitances and permit the determination of the important partial capacitances of the system. For example, $C_{C_1D_1}=(e/\Delta1-C_{C_1D_2}\Delta2/\Delta1)$ determines the capacitance between the main dot and its associated center gate. The interdot capacitance can be extracted directly from the relationship

$$C_{D_1D_2}=C_{\Sigma D_2}\frac{\Delta2}{\Delta1}, \tag{2}$$

where $C_{\Sigma D_2}$ is the sum of the partial capacitances to both electrodes and conducting dot. The electrode capacitances can be determined by the peak separations of the CBO's in an appropriate voltage sweep. Equation (2) yields the most important capacitance of the combined system and determines the particular form the phase diagram takes. For the conductance data shown in Fig. 2(a) we have used the above model to calculate the capacitances of the double-dot structure and we find that the interdot capacitance is approximately 100 aF. Significantly this value is 30–40 % of the total dot capacitances, which we estimate to be 330 aF and 260 aF for the main and second dot, respectively. The quality of this fit is demonstrated in Fig. 2(b) where the measured conductance maxima are plotted as a function of the two center-gate voltages and, in addition, the calculated phase boundaries are shown.

As discussed above only those phase boundaries corresponding to a change in the total electron number result in an increased conductance through the device. In fact, for $T=0$, the selection rule is even more restrictive. The addition of an extra electron to the second, nonconducting, dot is inevitably an activated transport process due to the negligible tunneling probability between the second dot and the 2D reservoirs. Qualitatively this behavior is clearly visible in the data of Fig. 2(a); the large conductance maxima observed correspond to the steep phase-boundaries of Fig. 3 (shown bold) where the occupancy of the main dot is changed by one. The boundaries where the occupancy of the second dot changes are much less distinct, while the boundaries corresponding to an internal redistribution of charge (shown dotted in Fig. 3) are not observed at all. Similar activated transport has been observed in the magnetic field dependence of the CBO's of a single quantum dot.[8,10] In fact the similarity between the two systems is expected in that the magnetic field induced condensation of the Landau levels into spatially separated conducting rings gives rise to a similar coupled system.

The significance of the phase diagram becomes most apparent when the interdot coupling is compared with the influence of a purely metallic electrode. The charge quantization in the nonconducting dot leads to definite jumps in the electrostatic potential that influence the main dot. This, of course, is the reason for the jumps of the conductance peaks observed in the phase diagram of Fig. 3. In this sense the electron number of the second dot can drastically modify the device conductance. The addition of an extra electron to the

second dot can switch the device conductance from a CB maximum to zero (at $T=0$) as is illustrated by the points X and Y in Fig. 3. In essence this electrostatically driven switching is not dissimilar to the proposed change in the ground state required for the operation of the cellular automata of Ref. 4.

Finally we turn our attention to the two limiting cases of extremely strong and extremely weak coupling between the dots. The latter case is illustrated in Fig. 4(a) where the device conductance is plotted as a function of the two center-gate voltages as in Fig. 2(a). Clearly the CBO's are almost unaffected by the second center-gate voltage and no jumps in the peak positions are visible. The two dots are essentially isolated from each other; the slight tilt which is observable in the data is due to the weak capacitative coupling between the main dot and the second center gate ($C_{C_2D_1}$) which we calculate to be approximately 1.9 aF. The other extreme occurs at significantly more positive finger-gate voltages (typically $V_{F_1}=V_{F_2}>-475$ mV) where the dots are in essence coupled to form one large dot structure. This situation is shown in Fig. 4(b); again the range of center-gate voltages considered is as in Fig. 2. The peak positions clearly shift as the second center-gate voltage is increased; however in this regime it is no longer possible to observe any jumps in the peak positions and the interdot capacitance is undefined.

In conclusion we have used the CBO's to investigate the capacitative coupling in a parallel quantum-dot structure. We have demonstrated that the conductance of the structure is extremely sensitive to the configuration of the nonconducting dot and that the addition of a single electron can drastically change the conductance of the device. Furthermore the observed conductance data yield a rich variety of different behaviors which can be substantially explained in terms of a classical capacitance model of the structure.

We gratefully acknowledge both financial assistance from the Deutsche-Forschungsgemeinschaft as well as profitable discussions with A.O. Govorov, S. Ulloa, and W. Zwerger.

*Present address: Department of Physics, University of Pennsylvania, Philadelphia, PA 19104.

[1] L.P. Kouwenhoven, A.T. Johnson, N.C. van der Vaart, A. van der Enden, and C.J.P.M. Harmans, Phys. Rev. Lett. **67**, 1626 (1991).

[2] H. Pothier, P. Lafrage, C. Urbina, D. Esteve, and M.H. Devoret, Europhys. Lett. **17**, 249 (1992).

[3] U. Meirav, M.A. Kastner, and S.J. Wind, Phys. Rev. Lett. **65**, 771 (1990).

[4] C.S. Lent, P.D. Tougaw, and W. Porod, Appl. Phys. Lett. **62**, 714 (1993).

[5] M. Kemerink and L.W. Molenkamp, Appl. Phys. Lett. **65**, 1012 (1994).

[6] R.H. Blick, R.J. Haug, J. Weis, D. Pfannkuche, K.v. Klitzing, and K. Eberl (unpublished).

[7] F.R. Waugh, M.J. Berry, D.J. Mar, R.M. Westervelt, K.C. Campman, and A.C. Gossard (unpublished).

[8] T. Heinzel, S. Manus, D.A. Wharam, J.P. Kotthaus, G. Böhm, W. Klein, G. Tränkle, and G. Weimann, Phys. Rev. B **50**, 15 113 (1994).

[9] A.K. Evans, L.I. Glazman, and B.I. Shklovskii, Phys. Rev. B **48**, 11 120 (1993).

[10] A.A.M. Staring, B.W. Alphenaar, H. van Houten, L.W. Molenkamp, O.J.A. Buyk, M.A.A. Mabesoone, and C.T. Foxon, Phys. Rev. B **46**, 12 869 (1992).